Chemistry Research Journal, 2021, 6(1):159-171

Available online www.chemrj.org

Research Article

ISSN: 2455-8990
CODEN(USA): CRJHA5

Capsicum baccatum var. *pendulum* waste used to capture Cr^{3+} from aqueous solutions

Amanda Alves Domingos Maia[a], André Henrique Rosa[a], Claudia Hitomi Watanabe[a], Paulo Sérgio Tonello[a], Leandro Cardoso de Morais[a,*]

[a]Institute of Science and Technology, São Paulo State University (UNESP) "Júlio de Mesquita Filho", Sorocaba, São Paulo, Brazil.
Av. Três de Março, 511, Alto da Boa Vista, 18087-180 – Sorocaba, São Paulo, Brazil.
Contact number + 55 (15) 3238-3400, Extension line: 3429 – Fax: +55 (15) 3228-2842
*Corresponding author
Email: leandro.cardoso@unesp.br (L.C. Morais)

Abstract Heavy metals are released into aquatic environments largely from various anthropogenic activities and pose a risk to public health because of their toxic and non-biodegradable nature. This study quantifies the biosorption of heavy metals on a red pepper waste used as biomass to biochar production and builds a wetland. The measurements of SEM show relevant alterations in the surfaces when different temperature values were applied. The FTIR analysis showed the intensity of thermal alteration of the biomass by higher temperatures. The samples exhibited high background intensity indicating a proportion of highly disordered materials in the form of amorphous carbon at this biomass. Thermal decomposition process presented reactions in parallel and series, which make thermal decomposition materials more complicated. The adsorption kinetics was found to follow pseudo-second-order rate kinetic model, with a good correlation (R^2> 0.99) and Langmuir isotherms.

Keywords Biosorption of heavy metal, red pepper waste, thermal decomposition of biomass, kinetic and isotherms study

Introduction

Contamination with organic and inorganic toxins occur worldwide [1], and the presence of heavy metals wastewater has posed many serious environmental problems due to their non-biodegradable properties and toxicity, even at low concentrations [2]. More environmentally acceptable alternatives to unsustainable waste disposal techniques for dealing with this problem have been sought [3]. The most commonly treatment methods are precipitation that is unfavorable when dealing with large volumes or low concentration [4]. Among these techniques, adsorption is generally regarded as an effective and economical method for wastewater treatment and is gaining ground over the conventional technologies [5,6]. Application of biochar as a potential adsorbent material in water decontamination has been increasingly concerned due to the current expensive methods of removing heavy metals from water [7,8]. Biochar are organic waste combusted under low oxygen conditions, resulting in a porous, low density and carbon rich material [9]. A large surface area and cation exchange capacities, determined by raw materials and pyrolysis temperatures, enables enhanced sorption to their surfaces [10]. Red pepper is an important spice and has been used

throughout the world [11] and is considered the second most exported vegetable, encompassing an annual worldwide production of 30 million tons in an acreage of 4 million ha [12].

Process of biochar production of red pepper waste can minimize different type of pollutants and thus it has a wider applicability in water pollution control. Activated carbon is undoubtedly considered as universal adsorbent for effluent treatment [13]. Furthermore, adsorption process has emerged as a cost effective and efficient alternative for water and wastewater treatment utilizing naturally occurring and agricultural waste materials as adsorbents as these are cheaper, renewable and abundantly available [14].

The purpose of this present study was to assess the ability of red pepper waste and his biochar to adsorb Cr ions from aqueous solutions.

Materials and Methods

Raw Material

Red pepper waste (RPW) used on this study was *Capsicum baccatum*var. *pendulum.* At the laboratory, the biomass was washed in tap water and dried by oven drying Solab model SL-100/42 at 105 °C to constant weight. After drying, the samples were ground in a Wiley mill, MA048 - Marconi, followed by sieving, Solotest sieve, NBR # 100 (0.149 mm).

Pyrolysis Experiments and Characterization

Pyrolysis experiments were performed in a muffle furnace (Quimis Q318S21) under atmospheric pressure and partially inert conditions. A sample of red pepper waste (RPW) weighing 0.6 g was placed in a porcelain crucible in semi-closed position and placed in a muffle furnace and heated at 250 °C, 350 °C and 450 °C. The surface morphology and elemental composition of the red pepper waste (RPW) and the biochars (BC) were examined by scanning electron microscopy (SEM), model JEOL JSM-6010LA Analytical. The analyses were performed on FTIR spectrophotometer (JASCO FT/IR-410), the detection and collection of spectrum range was 4000–400 cm^{-1} with 4 cm^{-1}spectral resolution and 128 accumulations for each sample was done. The diffuse reflectance accessory was utilized for powder samples. To evaluate the crystal structure of the samples were performed by a PANalytical X-ray diffractometer, model X'Pert PRO. The analysis operating conditions were: Kα of Cu as the source of X-Rays, with angle θ to 2θ, energy 40 kV 30 mA and the measurements were done within the range of 3s from 3°C to 65°C and step size of 0.05.

Thermal Analysis

Thermogravimetric analysis were carried out at heating rate 10°C/min, using a simultaneous DSC-TGA equipment, TA Instruments, model SDT Q600, from 25°C to 1000°C. Nitrogen was used as purge gas at a 120 ml/min flowrate. About (3 mg) of the biomass and biochar at 250 °C, 350 °C and 450 °C were used in alumina pans in each analysis. The TA Instruments software provides the thermogravimetry (TG) and derivative thermogravimetry (DTG) curves.

Biosorption Capacity

The biosorption capacity of the RPW and the BC to metal chromium was verified. Solutions of these metals were prepared from standard solutions (1,000 mg/L) in concentrations ranging from 2–4 mg/L. The biosorption experiments were carried out at 21 °C, at pH values of 3.5 and 6.0, by mixing 0.2 g of the sample with 250 ml of solutions. Aliquots were withdrawn and filtered. After filtration, the filtrate was analyzed by using an Inductively Coupled Plasma Optical Emission Spectrometer – ICP-OES (Agilent Technologies 700). The contact times of 5, 10, 15, 30, 45, 60 and 75min were observed and studied for further experimental analysis.

Isotherm Studies

The adsorption capacity and intensity were calculated by the Freundlich (1906) and Langmuir (1918) isotherms. The Langmuir isotherm model assumes a monolayer adsorption in a homogeneous surface having a finite number of adsorption sites. The model was expressed by the equation below:

$$Q_e = \frac{Q_m K_a C_e}{1+K_a C_e} \quad (1)$$

Where Q_e is the amount of solute adsorbed per unit weight of adsorbent at equilibrium (mg/g), Q_m the monolayer adsorption capacity(mg/g), K_a the Langmuir or equilibrium constant of adsorption (m/g) and C_e the equilibrium concentration (mg/L).

The linearized expression of the Langmuir equation is given by following the equation:

$$1/Q_e = \left(\frac{1}{K_a Q_m}\right)\left(\frac{1}{C_e}\right) + \left(\frac{1}{Q_m}\right) \quad (2)$$

In contrast, the Freundlich isotherm model assumes heterogeneous surface energy. The model was represented by the equation:

$$Q_e = K_f C_e^{\,1/n_f} \quad (3)$$

Where K_f is the Freundlich constant (mg/g) (L/mg)1/n, Q_e the amount of solute adsorbed per unit weight of adsorbent at equilibrium (mg/g), C_e the equilibrium concentration of the solute in the liquid phase (mg/L) and 1/nF heterogeneity factor.

The linearized expression of the Freundlich equation is given by following the equation

$$\log Q_e = \log K_f + \left(\frac{1}{n_f}\right)\log C_e \quad (4)$$

Kinetic Study

Pseudo-First Order Model

A kinetic model for sorption analysis is the pseudo- first order rate expression below:

$$dQ_t/d_t = K_1 (Q_e - Q_t) \quad (5)$$

Where K_1 is the rate constant of first order sorption (1/min), Q_e is the amount of solute sorbed at equilibrium (mg/g) and Q_t is amount of solute sorbed on the surface of the sorbent at any time t (mg/g).

The linearized form is as shown the following equation:

$$\log (Q_e - Q_t) = \log Q_t - \frac{K_1}{2.303} t \quad (6)$$

Pseudo-Second Order Model

$$dQ_t/d_t = K (Q_e - Q_t)^2 \quad (7)$$

Where K is the rate constant of sorption (g/mg min), Q_e is the amount of soluted sorbate sorbed at equilibrium (mg/g), Q_t is amount of soluted sorbate on the surface of the sorbent at any time t (mg/g).

$$\frac{t}{Q_t} = \frac{1}{K_2 Q_e 2} + \frac{1}{Q_e} t \quad (8)$$

Results and Discussion

Characterization of biomass and biochar

Initially the weight loss of BC with respect to the RPW was determined and the mass loss percentages obtained of the BC 250 °C, 350 °C and 450 °C were 45.97% (m/m), 63.28% (m/m) and 75.36% (m/m), respectively. The pyrolysis conditions and the type of raw material affected the properties of the biochar formed. The Biochar is composed by raw material carbonized, volatile material, ash and water, one part was easily degraded depending not only on the characteristics of the raw material but also of the pyrolysis conditions, especially the final production temperature.

The SEM measurements were a more direct form of establishing the chemical and morphological changes occurring on the surface of biomass and biochar. The SEM analysis showed that biomass has a surface with structured and heterogeneous pores. The surface of the RPW and BC shows a striated, flat surface with small cracks and holes [15].

The results obtained by SEM and XRD for different points shows variation in morphology and chemical composition for with an increasing pyrolysis temperature, there was a decrease in the particle size of the material and an increase in its porosity and can be observed at Figure 1. The analyses showed that the particles of RPW and BC with lignin were polygonal in shape with multiple fracture surfaces. Analysis of the biocharat 250 °C, 350 °C and 450 °C showed that the lignin present in biomass particles had softened, melted and fused into a mass of matrix and vesicles. The delignification caused by pyrolysis process promotes the formation of holes in the cell wall structure and therefore its surface appears more porous and brittle compared to the biomass [16]. The vesicles were the result of volatile gasses released at higher temperatures [17]. The XRD analysis presented carbon, nitrogen, oxygen, phosphorus, magnesium, calcium, chlorine, potassium, aluminum and sulfur. The pores in the bio-adsorbent greatly favored the diffusion and adsorption of metal ions.

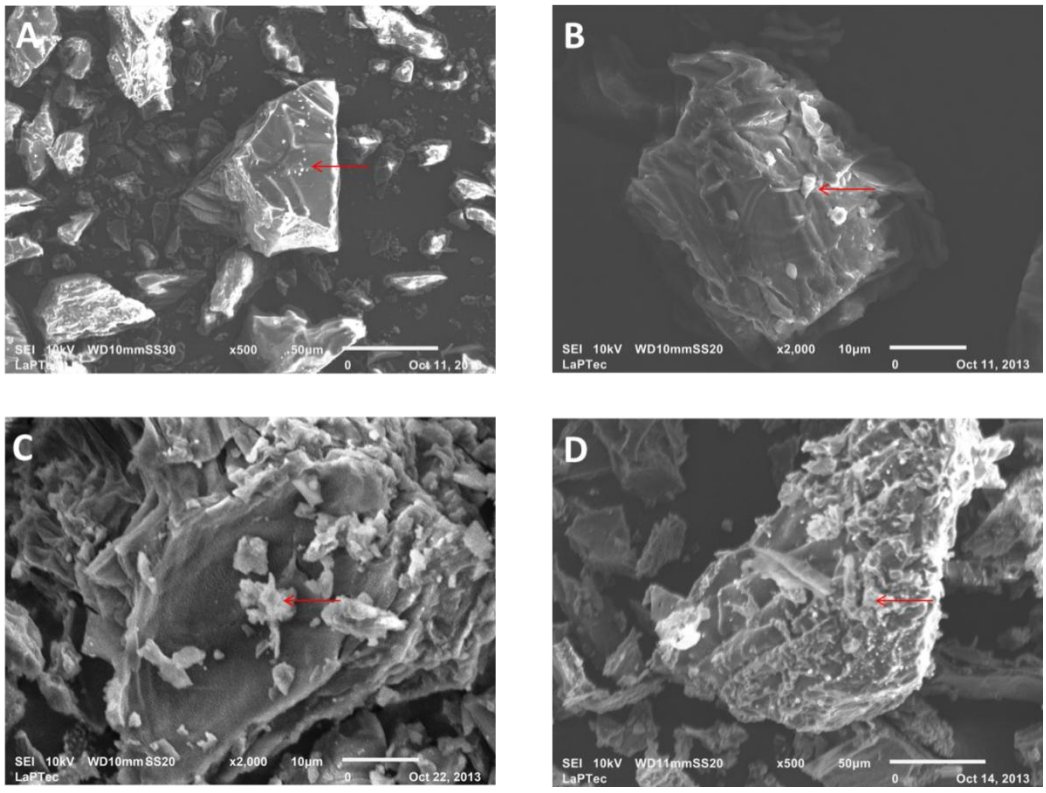

Figure 1: SEM images of red pepper powder (A), BC250°C (B), BC350°C (C) and BC450°C (D)

FTIR analysis was used to characterize the biomass according to its organic groups and the result is associated with lignin, an aromatic biopolymer of low regularity, crystallinity and optical activity. Clear differences can be detected in the infrared spectra and the FTIR spectra of biochar are characterized by broad bands creating difficulties in the differentiation of functional groups [18]. The composition of biocharmay indicate the intensity of thermal alteration of the biomass affected by higher temperatures [19]. The region between 3500 and 500 cm^{-1} is the more sensitive one to structural changes. According to [20], at the band 3560 cm^{-1} in the RPW there is a hydroxyl group (-OH) representing lignin and cellulose. The band 2900 cm^{-1} shows lignin and methyl group (-CH_3) [17] and ketone group (C=O) [20]. At the band about 1730 and 1736 cm^{-1} shows hemicellulose, acetyl group and ester. The lignin appears in bands 1600 cm^{-1} and 1500 cm^{-1} due to C = O in phenolic esters / lactones [21]. At range 1150 cm^{-1} and 609 cm^{-1} it was identified cellulose, (C-O), (C-O-C), (C-O), (C-H), (C-C) and aromatic ring [22]. The carbonyl groups probably formed by rearrangement and cyclization reactions of organic matter at high temperature are visible due to aliphatic compounds; the C–O stretching bands at 1200–1000 cm^{-1}.

Crystallinity is strongly influenced by the biomass composition. This biomass and his biochar at different temperatures presented the lowest relative crystallinity, because it has a higher content of hemicellulose and lignin, which are amorphous. Comparisons of the XRD patterns of the RPW with biochar suggest that the pyrolysis process did alter the crystal structure of the samples. The samples exhibited high background intensity indicating that the RPW contained a proportion of highly disordered materials in the form of amorphous carbon. It is suggested that carbon in biochar has an intermediate structure between graphite and amorphous structure. Biochar also contains significant amount of highly disordered material, amorphous carbon, which is responsible for the back ground intensity of the diffractions. The sample with lower content of lignin and hemicellulose were the biochar 450 °C that presented higher crystallinity. The diffractogram of RPW and biochar is summarized in Table 1. The amorphous structure of the samples can be observed about 5 and 35°.

Table 1: XRD patterns of RPW and Biochars

Sample	Formula	Elements
RPW	(Fe)	Iron
	(Al)	Aluminum
	(NaH_2PO_4)	Sodium phosphate
	KH_2PO_4	Potassium phosphate
	($C_8H_8O_{4)}$	o-vanillic acid
BC 250°C	(Fe)	Iron
	(Al)	Aluminum
	($H_6(P_2O_{62})$ $(H_2O)_{23,5}$)	Hydrogen Phosphate Hydrate
BC 350°C	(KCl)	Potassium chloride
	(C)	Carbon
	($C_{32}H_{28}N_7Cu_2O_{13}Pr$)	Nitrate
	($Li(Ni_{0,6}Co_{0,4})O_2$	Lithium Nickel and Cobalt Oxide
BC 450°C	($Fe_{19}Ni$)	Iron Nickel
	(Al)	Aluminum
	(Ni0)	Nickel Oxide
	$Ca(Fe^{2+},Mg)(CO_3)_2$),	Calcium Carbonate, Iron and Manganese

Thermal Analysis

Thermogravimetric (TG) was a rapid method for determining the temperature decomposition profile of a material and this stage are directly proportional to the amount of principle ingredients. The Figure 2 shows TG and DTG curves of RPW (A) and BC 250 °C (B), BC350 °C (C) and BC450 °C (D) at heating rate 10°C/min in nitrogen atmosphere. The pyrolysis process allows obtain three different phases: solid, liquid and gas and their composition is related to the temperature of the thermal treatment. The thermal decomposition of this biomass involved number of reactions in parallel and series, which make thermal decomposition materials more complicated. During the thermal decomposition process up to 1000 °C with the heating rate of 10 °C/min, around 90.86 wt.%, 62.67 wt.% , 89.75 wt.% and 33.24 wt.% of the biomass and BC250 °C, BC350 °C and BC450 °C was decomposed, respectively. The biochar formation was in a range of 200–550°C and by increasing the pyrolysis temperature, it was noted that an increased thermal stability of the material [23]. This biomass decomposition was divided into individual steps: water devolatilisation, hemicellulose, cellulose and lignin decomposition, because different stages of mass loss were observed for all the tested biomass and biochar. The first stage was due to the moisture, volatiles materials and hydrocarbons present at the sample [24]. This stage it was followed by thermal decomposition and a major loss of mass in the temperature range of 200 and 350 °C releasing the volatiles organics, characterizing the devolatilisation processes. About 350 °C shows thermal degradation of some carbohydrates such as cellulose and others about 400 °C can be observed a thermal decomposition of cellulose. The lignin decomposition begins at the below temperatures and up to 550 °C. Thermal decomposition of lignin can occurs in a temperature range from 200 °C to 900 °C, and mass loss rate is not as clear as in the case of hemicellulose and cellulose [24].

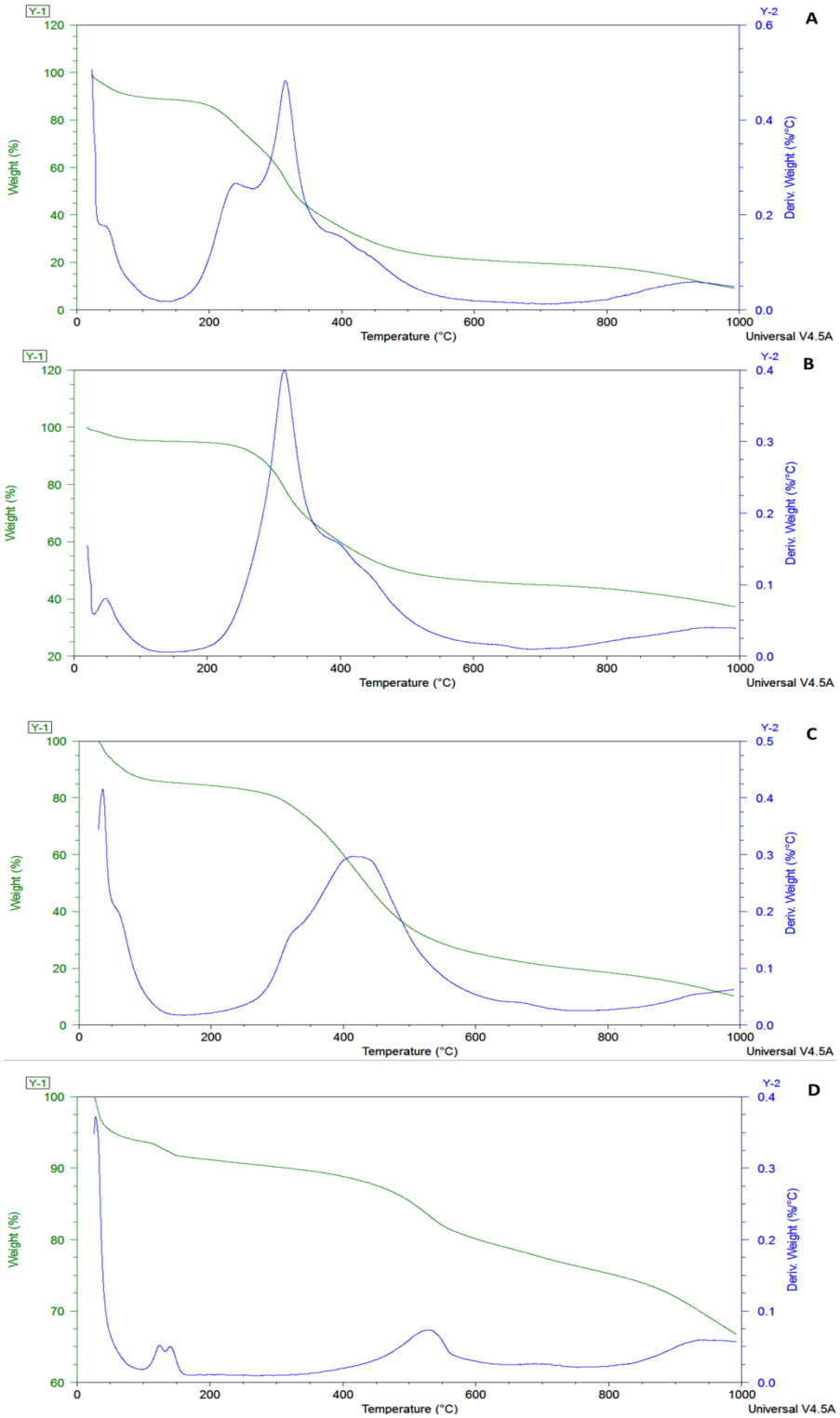

Figure 2: TG and DTG curves of RPW (A) and BC250 °C (B), BC350 °C (C) and BC450 °C (D) at heating rate 10°C/min in nitrogen atmosphere

Adsorption capacity

Langmuir and Freundlich isotherm models have widely been used in adsorption isotherm studies and were also used

in this work to fit the experimental isotherm data for Cr^{3+} adsorption on the adsorbents.

Table 2: Langmuir and Freundlich Isotherms at pH 3.5 and 6.0

	Langmuir								Freundlich					
	pH 3.5				pH 6.0				pH 3.5			pH 6.0		
Samples	**R^2**	**Qm**	**Ka**	**Rl**	**R^2**	**Qm**	**Ka**	**Rl**	**R^2**	**n_f**	**K_f**	**R^2**	**n_f**	**K_f**
RPW	0.96	3.20E-03	0.50	0.99	0.95	1.86E-03	1.31	1.00	0.98	2.56E-01	0.46	0.56	2.23E-01	0.33
BC250°C	0.97	2.50E-03	0.77	0.99	0.97	1.33E-02	0.12	1.00	0.55	1.95E-01	0.21	0.16	4.29E-01	0.57
BC350°C	0.76	2.40E-03	0.79	0.99	0.96	1.99E-02	0.08	0.99	0.4	1.94E-01	0.20	0.91	1.33E-01	0.03
BC450°C	0.58	1.50E-03	1.53	0.99	0.89	1.80E-03	1.48	0.99	0.13	2.30E-01	0.36	0.56	2.33E-01	0.39

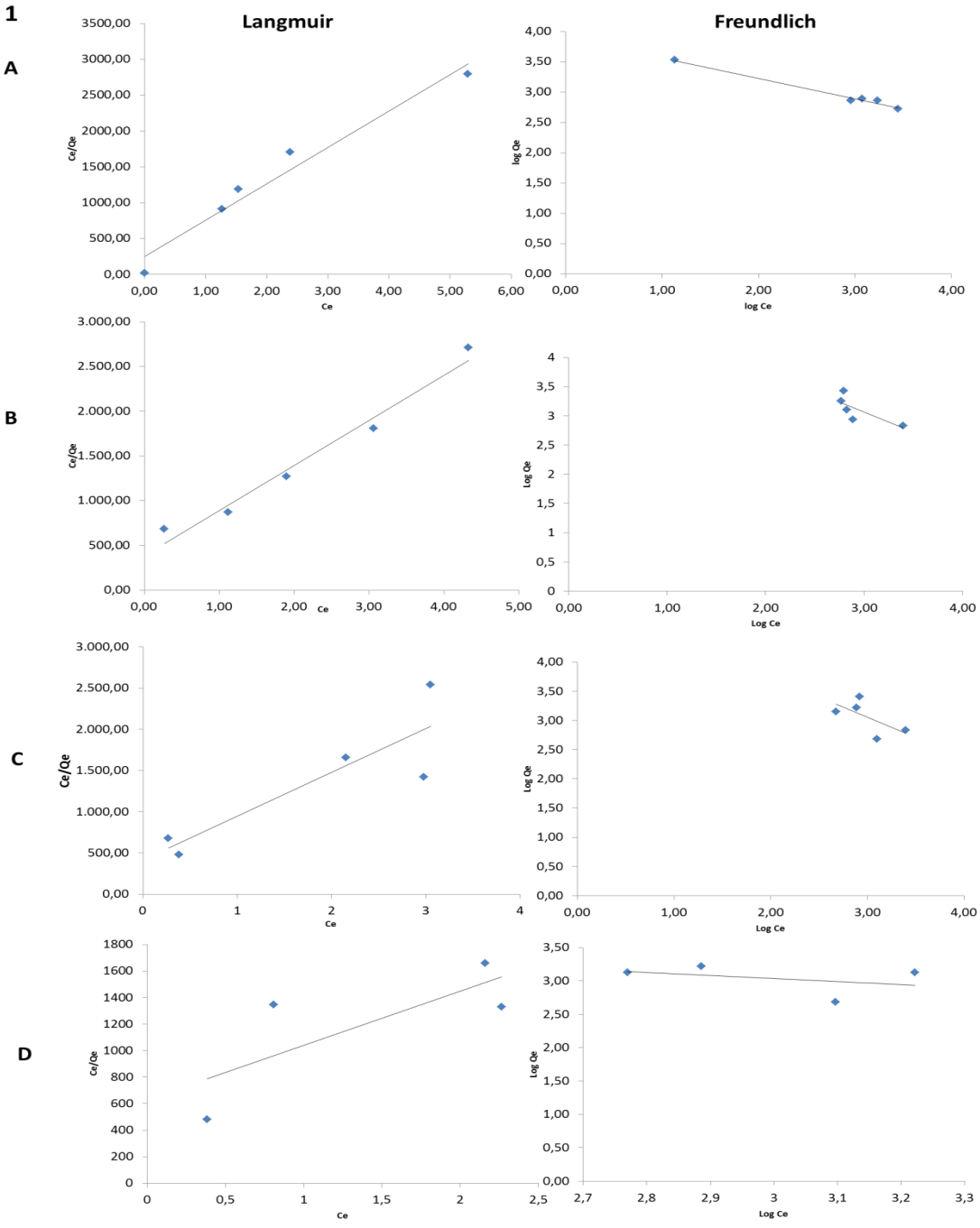

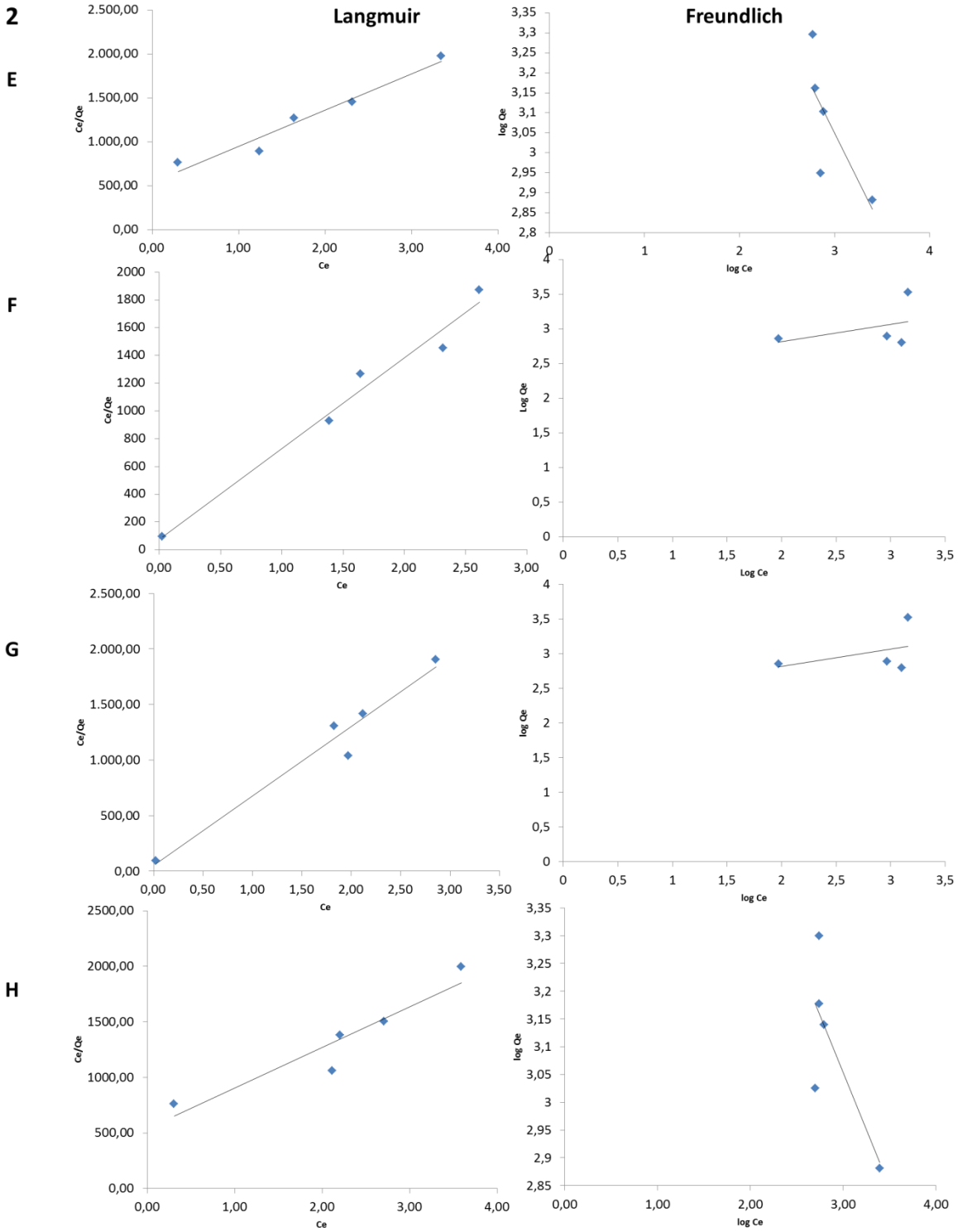

Figure 3: Langmuir and Freundlich Isotherms Models – 3.1-at pH 3.5 - RPW(A), BC250°C (B), BC350°C (C), BC450°C (D). 3.2- at pH 6.0 - RPW(E), BC250°C (F), BC350°C (G), BC450°C (H)

Table 2 and Figure 3 shows Langmuir and Freundlich Isotherms models at pH 3.5 and 6.0 results. The models were

tested and low determination coefficients R^2 from Freundlich demonstrated that the monolayer coverage of the adsorbent surface must be considered, according Langmuir model. The higher correlation coefficients (R_L^2) of the linearized Langmuir equation, 0.99 and 1.00 to pH 3.5 and 6.0, respectively, than those of the Freundlich equation (R_F^2), 0.46 and 0.57 to pH 3.5 and 6.0, respectively, indicate that the Langmuir model can fit the experimental results. Considering, pH 3.5 at Langmuir model, the RPW and the BC 250 °C, 350 °C and 450 °C presents greater results (R_l= 0.99) and at pH 6.0 the RPW and BC250 °C presents the better results (R_l= 1).The adsorption capacity of red pepper waste adsorbent for chromium was equal at pH 3.5 and 6.0 at 21 ºC, according to Langmuir model. At the same conditions, the biochar pyrolysed at 450 °C it was the worst adsorbent. According to Freundlich model, the red pepper waste adsorbent was the better at pH 3.5 and BC 350 °C at pH 6.0 and BC 250°C and 350 °C were the worst adsorbent at pH 3.5 and 6.0, respectively.

The pH value of the solution had an important controlling parameter in the adsorption process. The heavy metal cations are usually released under circumstances of acidic conditions. The adsorption capacity of heavy metal onto RPW and Biochar increases significantly with increasing pH. The lower value (pH=3.5) was chosen because it was at or near the end of the first adsorption stage and the higher pH (6.0) corresponded to adsorption in the second stage and the temperature dependence of adsorption at this pH is weaker. At acidic pH, a high electrostatic attraction exists between the positively charged surface of the adsorbent and heavy metal [25].

The inconsistency in literature regarding the influence of pH on adsorption seems to indicate that the way pH would alter the adsorption of metal ions to biomass varies with the type of adsorbents and adsorbates. When the equilibrium time increased, the amount of adsorption also increased. The maximum adsorption of chromium onto RPW and Biochar was observed at 75 minutes and it is thus fixed as the optimum contact time. The percent adsorption is minimum at pH 3.5 and the maximum adsorption occurs at pH 6. The minimum adsorption at low pH may be due to the fact that high concentration and high mobility of H^+ ions, the hydrogen ions are preferentially adsorbed compared to Cr ions. At the Figure 4 and Table 3 is possible to observe the Pseudo-Second Order Kinetic Model at different pH and concentration. The correlation coefficients for the pseudo-second order kinetic model (R^2) were higher (0.74 and 0.99 at pH 3.5 and 0.96 and 0.99 at pH 6.0) than those of the pseudo-first order kinetic model (R^2) (0.64 and 0.98 at pH 3.5 and 0.8 and 0.98 at pH 6.0). These results suggest that the adsorption kinetics of Cr on the adsorbent are well-represented by the pseudo-second order kinetic model. Therefore, the adsorption of Cr on the adsorbent is dominated by a chemical adsorption process and ion exchange. Adsorption data was modeled using the Langmuir and Freundlich adsorption. These results indicate that the adsorption properties of adsorbent can be further improved by tailoring the chemical and physical structure. The findings presented here suggest that, besides the amount of ligands, porous structure is also an important factor that determines the adsorption properties.

Table 3A – Pseudo-Second and Pseudo-First Order Kinetic Models at pH 3.5 and [2.0 mg/L], [2.5 mg/L], [3.0 mg/L], [3.5 mg/L] and [4.0 mg/L] concentrations

A		**Pseudo-Second Order**			**Pseudo-First Order**		
		pH 3.5					
Concentration	**Samples**						
		Q_e	**K_2**	**R^2**	**Q_e**	**K_1**	**R^2**
	RPW	7.14E+02	7.00E-04	0.99	7.69E+02	2.00E-02	0.76
2.0 mg/L	**BC250°C**	7.69E+02	3.67E-04	0.99	6.67E+02	3.92E-02	0.98
	BC350°C	1.25E+03	1.07E-03	0.99	4.76E+02	1.54E-02	0.89
	BC450°C	1.25E+03	8.00E-04	0.99	5.88E+02	1.89E-02	0.92
		Q_e	**K_2**	**R^2**	**Q_e**	**K_1**	**R^2**
	RPW	7.69E+02	1.48E-04	0.97	7.69E+02	1.89E-02	0.92
2.5 mg/L	**BC250°C**	6.67E+02	2.16E-04	0.98	6.67E+02	1.91E-02	0.94
	BC350°C	4.76E+02	1.84E-03	0.99	4.76E+02	4.81E-02	0.88
	BC450°C	5.88E+02	2.89E-04	0.99	5.88E+02	3.41E-02	0.95
		Q_e	**K_2**	**R^2**	**Q_e**	**K_1**	**R^2**
3.0 mg/L	**RPW**	7.14E+02	3.63E-04	0.99	7.69E+02	3.62E-02	0.91

	BC250°C	5.88E+02	3.25E-04	0.99	6.67E+02	2.69E-02	0.64
	BC350°C	7.69E+02	2.73E-04	0.99	7.69E+02	2.05E-02	0.89
	BC450°C	2.00E+03	1.19E-04	0.99	2.00E+03	2.21E-02	0.91
		Q_e	**K_2**	**R^2**	**Q_e**	**K_1**	**R^2**
	RPW	3.33E+03	1.27E-05	0.99	3.33E+03	1.59E-02	0.93
3.5 mg/L	**BC250°C**	2.50E+03	1.40E-05	0.97	2.50E+03	1.77E-02	0.98
	BC350°C	2.50E+03	7.27E-05	0.99	2.50E+03	2.81E-02	0.90
	BC450°C	1.67E+03	8.57E-05	0.98	1.67E+03	5.02E-02	0.93
		Q_e	**K_2**	**R^2**	**Q_e**	**K_1**	**R^2**
	RPW	5.26E+02	6.45E-04	0.99	5.26E+02	2.83E-02	0.76
4.0 mg/L	**BC250°C**	6.25E+02	3.32E-04	0.97	6.25E+02	3.39E-02	0.94
	BC350°C	8.33E+02	7.74E-05	0.89	8.33E+02	2.76E-02	0.87
	BC450°C	1.25E+04	2.13E-06	0.74	1.25E+04	8.98E-03	0.89

Table 3B: Pseudo-Second and Pseudo-First Order Kinetic Models at pH 6.0 and [2.0 mg/L], [2.5 mg/L], [3.0 mg/L], [3.5 mg/L] and [4.0 mg/L] concentrations

B		**Pseudo-Second Order**			**Pseudo-First Order**		
		pH 6.0					
Concentration	**Samples**						
		Q_e	**K_2**	**R^2**	**Q_e**	**K_1**	**R^2**
	RPW	7.14E+02	7.00E-04	0.99	7.14E+02	9.90E-03	0.92
2.0 mg/L	**BC250°C**	6.67E+02	5.11E-04	0.99	6.67E+02	2.30E-04	0.88
	BC350°C	5.26E+02	6.12E-04	0.99	5.26E+02	3.57E-02	0.98
	BC450°C	5.00E+02	6.90E-04	0.99	5.00E+02	3.16E-02	0.81
		Q_e	**K_2**	**R^2**	**Q_e**	**K_1**	**R^2**
	RPW	7.69E+02	1.82E-04	0.99	7.69E+02	2.92E-02	0.93
2.5 mg/L	**BC250°C**	7.69E+02	1.52E-04	0.99	7.69E+02	2.67E-02	0.97
	BC350°C	7.14E+02	1.85E-04	0.99	7.14E+02	2.12E-03	0.89
	BC450°C	6.25E+02	2.94E-04	0.99	6.25E+02	3.32E-02	0.94
		Q_e	**K_2**	**R^2**	**Q_e**	**K_1**	**R^2**
	RPW	6.25E+02	5.12E-04	0.99	6.25E+02	5.69E-02	0.94
3.0 mg/L	**BC250°C**	6.25E+02	1.70E-04	0.99	6.25E+02	5.23E-02	0.8
	BC350°C	6.67E+02	2.30E-04	0.99	6.67E+02	4.12E-02	0.84
	BC450°C	5.56E+02	4.32E-04	0.99	5.56E+02	3.62E-02	0.91
		Q_e	**K_2**	**R^2**	**Q_e**	**K_1**	**R^2**
	RPW	3.33E+03	9.00E-06	0.98	3.33E+03	1.77E-02	0.98
3.5 mg/L	**BC250°C**	3.33E+03	4.04E-06	0.98	3.33E+03	9.67E-03	0.92
	BC350°C	3.33E+03	5.92E-06	0.97	3.33E+03	1.17E-02	0.93
	BC450°C	2.50E+03	3.19E+08	0.99	2.50E+03	1.31E-02	0.87
		Q_e	**K_2**	**R^2**	**Q_e**	**K_1**	**R^2**
	RPW	5.88E+02	3.18E-04	0.96	5.88E+02	1.59E-02	0.92
4.0 mg/L	**BC250°C**	7.14E+02	1.50E-04	0.96	7.14E+02	2.88E-02	0.81
	BC350°C	6.67E+02	2.88E-04	0.99	6.67E+02	3.55E-02	0.81
	BC450°C	5.56E+02	7.90E-04	0.99	5.56E+02	3.66E-02	0.92

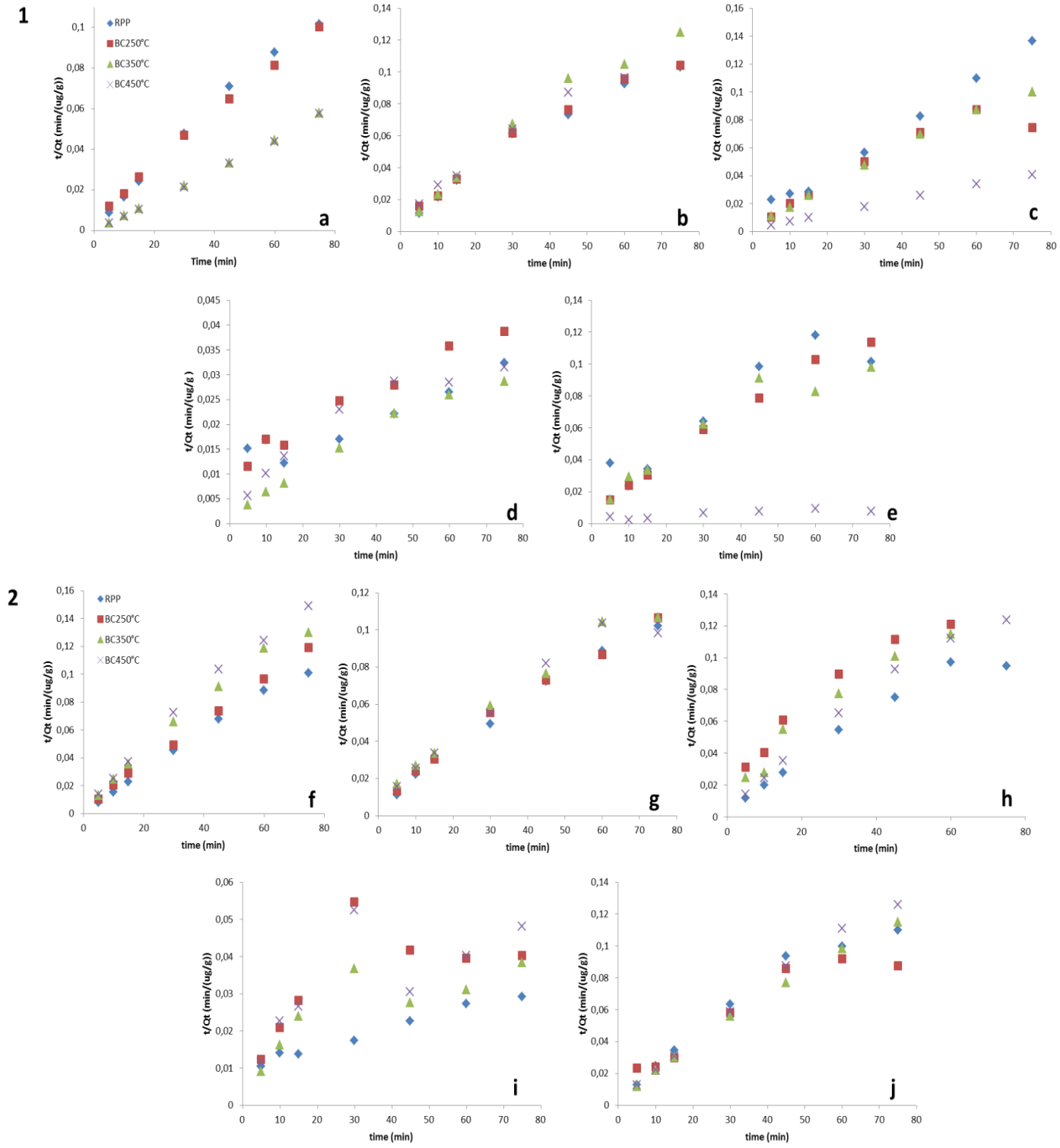

Figure 4: Pseudo-Second Order Kinetic Model – 4.1-at pH 3.5 and [2.0 mg/L] (a), [2.5 mg/L] (b), [3.0 mg/L] (c), [3.5 mg/L] (d) and [4.0 mg/L] (e) concentrations; 4.2- at pH 6.0 and [2.0 mg/L] (f), [2.5 mg/L] (g), [3.0 mg/L] (h), [3.5 mg/L] (i) and [4.0 mg/L] (j) concentrations.

Conclusion

The purpose of the present study was to evaluate the removal efficiency of chromium from aqueous solutions red pepper waste. Pyrolysis experiments and characterization of the samples were relevant to understand the adsorption process. The red pepper waste used at this study was mainly composed of carbon, nitrogen, oxygen, phosphorus, magnesium, calcium, chlorine, potassium, aluminum and sulfur and pores in the bio-adsorbent greatly favored the diffusion and adsorption of metal ions. FTIR analysis identified lignin, cellulose and hemicellulose at different bands and XRD patterns suggest that the pyrolysis process did alter the crystal structure of all the samples. Thermal analysis shows that thermal decomposition of the biomass studied is a complex phenomenon which is due to different structural and elemental characteristics along with the type of reactive atmosphere. The results of present study reveal that the red pepper waste can be beneficially utilized as an effective biosorbent for the removal of chromium from aqueous solutions. Kinetic studies suggest that chromium adsorption on red pepper adsorbent could be described more favorably by the pseudo-second-order kinetic model and Langmuir Isotherms model.

Acknowledgements

The authors acknowledge the financial support provided by Brazilian Research Agencies: CAPES, CNPq and FAPESP.

References

[1]. Mench, M., Lepp, N., Bert, V., Schwitzguébel, J., Gawronski, S. W., Schroder, P., (2010). Successes and Limitations of Phytotechnologies at Field Scale : Outcomes, Assessment and Outlook from COST Action 859 Successes and limitations of phytotechnologies at field scale : outcomes, assessment and outlook from COST Action 859. J Soils Sediments, 10, 1039–1070.

[2]. Vilar, J. P. V, Botelho, M. S. C., Boaventura, A. R. R., (2007). Copper desorption from Gelidium algal biomass. Water Res., 41, 1569–1579.

[3]. Beesley, L., Moreno-Jiménez, E., Gomez-Eyles, J. L., Harris, E., Robinson, B., Sizmur, T., (2011). A review of biochars ' potential role in the remediation , revegetation and restoration of contaminated soils. Environ. Pollut. 159, 3269–3282.

[4]. Dabrowski, A., Hubicki, Z., Podkóscielny, P., Robens, E., (2004). Selective removal of the heavy metal ions from waters and industrial wastewaters by ion-exchange method. Chemosphere, 56, p. 91–106.

[5]. Fenandes, J.O., Bernardino, C.A.R., Mahler, C.F., Santelli, R.E., Braz, B.F., Borges, R.C., Veloso, M.C.C., Romeiro, G.A., Cincotto, F.H., (2021). Biochar generatedfrom agro-industry sugarcane residue by low temperature pyrolysis utilized as an adsorption agent for the removal of Thiamethoxam pesticide in wastewater. Water Air Soil Pollut., 67, 232.

[6]. Kampalanonwat, P., Supaphol, P., (2014). The Study of Competitive Adsorption of Heavy Metal Ions from Aqueous Solution by Aminated Polyacrylonitrile Nanofiber Mats. Energy Procedia, 56, 142–151.

[7]. Arami, M., Limaee, N.Y., Mahmoodi, N. M., Tabrizi, N. S., (2005). Removal of dyes from colored textile wastewater by orange peel adsorbent: Equilibrium and kinetic studies. J. Colloid Interface Sci. 288, 371–376.

[8]. Lehmann, J., (2007). A handful of carbon. Nature, 447, 143–144.

[9]. Ogundiran, M. B., Lawal, O. O., Adejumo, S. A., (2015). Stabilisation of Pb in Pb Smelting Slag-Contaminated Soil by Compost-Modified Biochars and Their Effects on Maize Plant Growth. J Environ. Protec., 6, 771–780.

[10]. Farrell, M., Jones, D. L., (2010). Use of composts in the remediation of heavy metal contaminated soil. J. Hazard. Mater. 175, 575–582.

[11]. Lee, J. H., Sung, T.H., Lee, K.T., Kim, M.R., (2004). Effect of Gamma-irradiation on Color , Pungency , and Volatiles of Korean Red Pepper Powder. J. Food Sci., 69.

[12]. Freibauer, A., Mathijs, E., Brunori, G., Damianova, Z., Faroult, E., Gomis, J., Girona, I., O'Brien, L., Treyer, S., (2011). Sustainable food consumption and production in a resource-constrained world. 3. ed.

Belgium, 236.

[13]. Bhatnagar, A., Sillanpää, M., (2010). Utilization of agro-industrial and municipal waste materials as potential adsorbents for water treatment — A review. Chem. Eng. J., 157, 277–296.

[14]. Ferda, G., (2012). Adsorption study on orange peel: Removal of Ni(II) ions from aqueous solution. Afr. J. Biotechnol. 11, 1250–1258.

[15]. Velásquez, P., Leinen, D., Pascual, J., Ramos-Barrado, J. R., Grez, P., Gómez, H., Schrebler, R., Del Río, R., Córdova, R., (2005). A chemical, morphological, and electrochemical (XPS, SEM/EDX, CV, and EIS) analysis of electrochemically modified electrode surfaces of natural chalcopyrite ($CuFeS_2$) and pyrite (FeS_2) in alkaline solutions. J. Phys. Chem, 109, 4977–4988.

[16]. Lima, M. A., Oliveira-neto, M., Kadowaki, A. S., Rosseto, F. R., Prates, E. T., Squina, F. M., Adriana, F., Leme, P., Skaf, M. S., Polikarpov, I., (2013). *Aspergillus niger* beta-glucosidase has a cellulase-like tadpole molecular shape: insights into GH3 beta-glucosidases structure and function. J. Biol. Chem., 288, 32991–33005.

[17]. Sharma, R. K., Wooten, J. B., Baliga, V. L., Lin, X., Geoffrey Chan, W., Hajaligol, M. R., (2004). Characterization of chars from pyrolysis of lignin. Fuel, 83, 1469–1482.

[18]. Kaal, J., Martínez, A. C., Reyes, O., Soliño, M., (2012). Molecular characterization of Ulex europaeus biochar obtained from laboratory heat treatment experiments - A pyrolysis-GC/MS study. J. Anal. Appl. Pyrolysis, 95, 205–212.

[19]. Francioso, O., Sanchez-Cortes, S., Bonora, S., Lorena, M., Certini, G., (2011). Structural characterization of charcoal size-fractions from a burnt Pinus pinea forest by FT-IR , Raman and surface-enhanced Raman spectroscopies. J. Mol. Struct. 994, 155–162.

[20]. Silverstein, R., Webster, F., (1998). Spectrometric Identification of Organic Compounds.

[21]. Potthast, A., Rosenau, T., Kosma, P., Saariaho, A. M., Vuorinen, T., (2005). On the nature of carbonyl groups in cellulosic pulps. Cellulose, 12, 43–50.

[22]. Suárez-García, F., Martínez-Alonso, A, Tascón, J. M., (2002). A comparative study of the thermal decomposition of apple pulp in the absence and presence of phosphoric acid. Polym. Degrad. Stab., 75, 375–383.

[23]. Santos, C. M., Dweck, J., Viotto, R.S., Rosa, A. H., Morais, LC., (2015). Application of orange peel waste in the production of solid biofuels and biosorbents. Bioresour. Technol. 196, 469–479.

[24]. Maia, A.A.D., Morais, L.C., (2016).Kinetic parameters of red pepper waste as biomass to solid biofuel. Bioresour. Technol. 204, 157–163.

[25]. Özcan, A. S., Özcan, A., (2004). Adsorption of acid dyes from aqueous solutions onto acid-activated bentonite. J. Colloid Interface Sci., 276, 39–46.